

## Theory of self-assembly-driven nematic liquid crystals revised

C. De Michele

To cite this article: C. De Michele (2019): Theory of self-assembly-driven nematic liquid crystals revised, Liquid Crystals, DOI: [10.1080/02678292.2019.1645366](https://doi.org/10.1080/02678292.2019.1645366)

To link to this article: <https://doi.org/10.1080/02678292.2019.1645366>



Published online: 27 Aug 2019.



Submit your article to this journal [↗](#)



Article views: 24



View related articles [↗](#)



View Crossmark data [↗](#)

# Theory of self-assembly-driven nematic liquid crystals revised

C. De Michele

Dipartimento di Fisica, "Sapienza" Università di Roma, Rome, Italy

## ABSTRACT

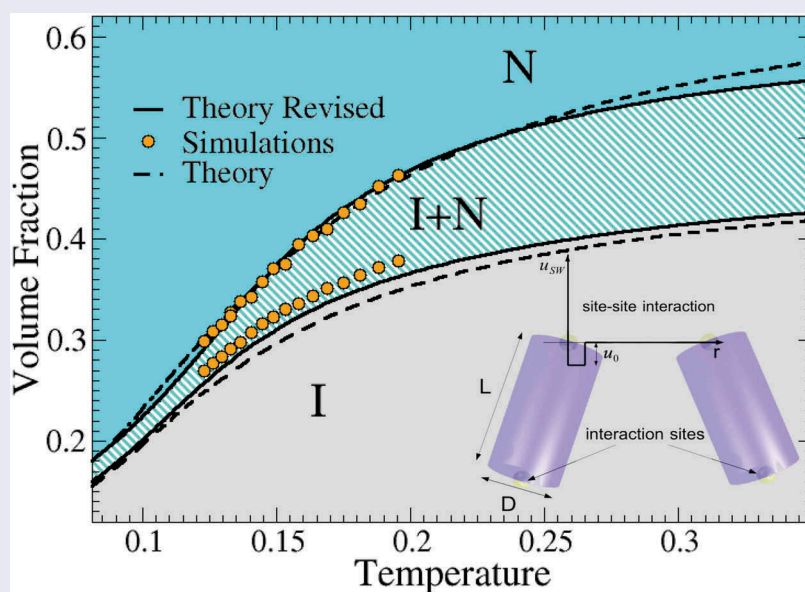
Concentrated solutions of short blunt-ended DNA duplexes at room temperature can form liquid crystal phases due to stacking interactions between duplex terminals which induce the aggregation of the duplexes into semi-flexible linear chains. Mesophases observed in these systems include nematic, columnar and cholesteric ones. This experimental system is just one of many examples, where liquid crystals ordering emerges as a result of molecular self-assembly into linear chains. In the attempt to go beyond a simple Onsager theoretical approach to understand the thermodynamic behavior of this system, we introduced some years ago a general theoretical description, which models the isotropic-nematic transition by properly taking into account molecular self-assembly, and we carefully verified the theoretical predictions against numerical simulations of patchy hard cylinders. Here, we provide a revised version of the theory in the attempt of understanding which assumptions are worth to be improved. In particular, we focus on the Parsons-Lee approximation and the modeling of orientational entropy. We compare the results from the revised version of the theory against original ones, showing that the present version of the theory is able to capture more accurately the phase boundaries of the isotropic-nematic transition.

## ARTICLE HISTORY

Received 1 March 2019

## KEYWORDS

Theory; lyotropic liquid crystals; self-assembly; phase diagram; monte carlo simulations



## 1. Introduction

The spontaneous formation, through free energy minimization of reversible aggregates from basic building blocks, is called self-assembly. Since building block size can vary from few angstroms to microns, self-assembly is rather ubiquitous in nature. In addition, the interactions between building blocks can be conveniently tuned, so that through self-

assembly new materials with controlled physical properties can be designed. It is for these reasons that self-assembly is of interest in several fields, such as material science, soft matter and biophysics [1–3].

A specific, but nonetheless less relevant, self-assembly process is the formation of filamentous semi-flexible aggregates induced by the anisotropy of attractive interactions between the constituent building blocks.

Examples are provided by micellar systems [4–6], formation of fibers and fibrils [7–10], solutions of short [11–18] and long B-DNA [19–22], chromonics [23–29] and inorganic nanoparticles [30–33].

In these systems liquid crystal (LC) phases build up above a critical concentration, if the filamentous aggregates are sufficiently stiff. In order to grasp a physical understanding of this complex behavior, building on the venerable Onsager theory, we developed some years ago a novel theoretical approach for these self-assembly-driven LCs. Noticeably, our theory contains no adjustable nor fitting parameters. Predictions for the isotropic-nematic transition have been carefully tested through computer simulations for polymerizing hard cylinders [34], patchy cylinder-like superquadrics [35], a realistic DNA coarse-grained model [36], patchy bent cylinders [37], bifunctional spheres [38] and patchy disks [39]. The theoretical treatment has been also extended to the calculations of chiral strength and elastic constants [39,40]. In this theoretical treatment, the contribution of higher order virial terms to free energy has been accounted for by the Parsons-Lee (PL) decoupling approximation, while the modeling of the orientational contribution to the free energy depends on a constant (i.e. independent of thermodynamic state point) parameter which discriminates the regimes of rigid and fully flexible chains.

In this manuscript, we discuss further these two approximations used in the theory and we suggest a possible way to improve them. The PL approximation is not accurate at moderate and large packing fractions, since in the form used in the original theoretical treatment it has been used without taking into account the effective volume occupied by a chain, which is larger than the total volume occupied by its constituent monomers. Concerning the constant parameter which acts as threshold separating stiff and fully flexible chains, in Ref [41], it has been observed that it should depend on the orientational ordering if one wants to explain some experimental findings on the phase behavior of a suspension of short amyloid fibrils. In Ref [41], it has been also noted that this parameter should be comparable with, rather than the persistence length, the deflection length, as defined and discussed in Refs [42,43]. In the present manuscript a first attempt to go beyond these two approximations will be provided, which should be intended as a guide for further future improvements of the theory.

In Sec. 2 we will illustrate briefly the patchy cylinder model which will be used to test the theoretical predictions. Sec. 3 provides an account of the theoretical treatment where we discuss a possible way to improve the approximations discussed so far. In Sec. 4 we show the theoretical predictions of the novel theoretical

treatment and we compare them with the results for patchy hard cylinder reported in Ref [34]. Finally, in Sec. 5 the conclusions will be drawn.

## 2. Model

For testing the revised version of the theory developed in Refs [35], we consider the same model adopted in Ref [34], which will be illustrated briefly in the following. We consider hard cylinders (HC) of length  $L$  and diameter  $D$ , which are complemented with two attractive sites on their bases (Figure 1).

These two attractive sites are placed along the symmetry axis of the HC at a distance  $L/2 + 0.15D/2$  from its center of mass, so that no branching can occur in the system. Attractive sites which belong to distinct HCs interact via the following square-well (SW) potential  $u_{SW}$ :

$$\beta u_{SW} = \begin{cases} -\beta u_0 & \text{if } r \leq \delta \\ 0 & \text{if } r > \delta \end{cases} \quad (1)$$

where  $r$  is the distance between the interacting sites,  $\delta = 0.25D$  is the interaction range,  $\beta u_0$  is the ratio between the binding energy  $u_0$  and the thermal energy  $k_B T = \beta^{-1}$ , with  $k_B$  the Boltzmann constant. It is convenient to define an adimensional temperature  $T^* = k_B T / u_0$ , which will be used in the following. Note that  $u_0$  is assumed to be independent of aggregate size, which is equivalent to assume that the self-

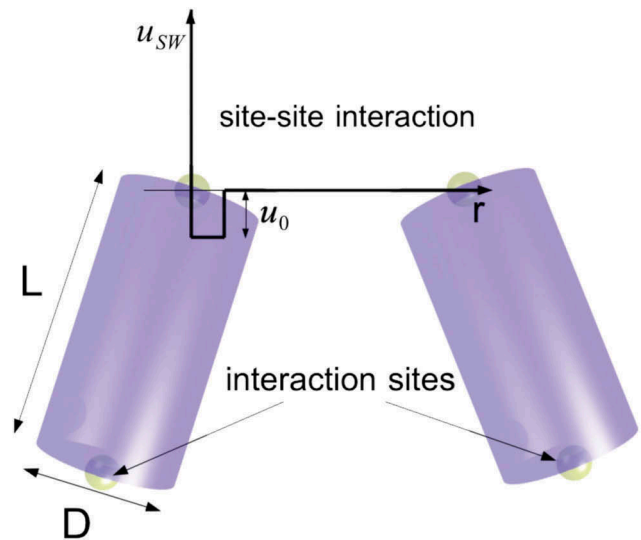


**Figure 1.** (Colour online) Patchy hard cylinder model used in the theoretical calculations.  $D$  and  $L$  diameter and length of cylinders respectively. The centers of the two small yellow spheres placed on the bases of the cylinders are the sites interacting via a square-well potential. The diameter of the yellow spheres coincides with the interaction range (i.e. the well width), while the depth of the well  $u_0$  is the binding energy.

assembly process is isodesmic [44,45].

### 3. Theory

In the systems, which we are considering in the present study, particles aggregate to form chains of various lengths. Hence, the system is a polydisperse mixture of semi-flexible polymers, which continuously change their lengths, by merging with other polymers or breaking of the constituting bonds. The original theoretical approach developed in Ref [35], followed the work of van der Schoot and Cates [6,46] and its extension to higher volume fractions with the use of the Parsons-Lee approximation [47,48] as suggested by Kuriabova *et al.* [49]. For a polydisperse mixture of self-assembling linear aggregates, the Helmholtz free energy  $F$  can be naturally expressed as a functional of the number density of aggregates  $\nu(l)$ , where  $l$  is the length (or number of monomers) of the aggregate to which a monomer belongs. The function  $\nu(l)$  has to obey the normalization condition

$$\sum_l l\nu(l) = \rho \quad (2)$$

where  $\rho = N/V$ , with  $N$  the number of monomers and  $V$  the volume, is the number density of monomers. In the following we assume an exponential aggregate length distribution, i.e.

$$\nu(l) = \rho M^{l-1} / (M-1)^{l+1} \quad (3)$$

with  $M$  the average number of monomers in the aggregate, i.e.

$$M = \frac{\sum_1^\infty l\rho(l)}{\sum_1^\infty \rho(l)}. \quad (4)$$

The Helmholtz free energy comprises the following contributions [34,35,40]:

$$F = F^{id} + F^{st} + F^{or} + F^{excl} \quad (5)$$

In this equation  $F^{id}$  is the free energy of an ideal gas composed of a polydisperse mixture of chains with chain length distribution  $\nu(l)$ , where  $v_d = LD^2\pi/4$  is the volume of a monomer. This ideal gas contribution can be written in terms of the chain length distribution  $\nu(l)$  as follows:

$$F^{id} = V\beta^{-1} \sum_{l=1}^\infty \nu(l) \{ \ln[v_d \nu(l)] - 1 \}. \quad (6)$$

The term,  $F^{st}$ , is the stacking free energy, which accounts for monomer aggregation. Expressed in terms of the chain length distribution  $\nu(l)$  it takes the following form:

$$F^{st} = V\beta^{-1} \Delta(T) \sum_{l=1}^\infty (l-1)\nu(l) \quad (7)$$

where  $\Delta(T)$  is the bonding free energy [35,36], i.e.

$$\Delta(T) = -(\beta u_0 + \sigma_b) \quad (8)$$

with  $u_0$  the (positive) stacking energy and  $\sigma_b$  the entropic free energy penalty for bonding, i.e. the contribution to free energy due to the entropy which is lost by forming a single bond. The quantity  $\sigma_b$  can be expressed in terms of the bonding volume  $V_b$ , which has been introduced within the Wertheim theory [50], as follows:

$$\sigma_b = \ln\left(\frac{2V_b}{v_d}\right) \quad (9)$$

The bonding volume  $V_b$  can be conveniently calculated via Monte Carlo (MC) integration as described in detail in Ref [35]. For the present model  $V_b$  has been already evaluated in Ref [34].

In passing, we note that if the term  $F^{st}$  is missing in the free energy, i.e. there is no aggregation between molecules, other theories have been also proposed to deal with aggregate flexibility, which rely on other approaches than that of Khokhlov and Semenov [51,52].

$F^{or}$  accounts for the orientational entropy lost due to the alignment of the chains in the nematic phase (including the contribution due to their flexibility). An analytic expression for this contribution will be proposed and discussed in Sec. 3.2

The fourth term  $F^{excl}$  arises from excluded volume interactions between chains and thus it comprises a sum over  $\nu_{excl}(l, l')$ , which is the excluded volume of two chains with lengths  $l$  and  $l'$ , i.e.

$$F^{excl} = V\beta^{-1} \frac{\eta(\zeta\phi)}{2} \sum_l \sum_{l'} \nu(l)\nu(l') \bar{v}^{excl}(l, l') \quad (10)$$

where  $\eta(\zeta\phi)$  is a modified Parsons-Lee factor [47,48] introduced to account for higher order terms in the virial expansion, with

$$\eta(x) = \frac{1}{4} \frac{4-3x}{(1-x)^2} \quad (11)$$

and the system volume fraction  $\phi = \rho v_d$  is scaled by the factor  $\zeta$ , as suggested in Ref [38]. The motivation for introducing the factor  $\zeta$  is that the so-called effective molecular volume of non-convex chains is expected to be larger than the sum of the volume of the constituent monomers, as suggested and discussed in Ref [53], where a system of linear fused hard sphere chains was studied. In the present approach  $\zeta$  has to be regarded

as an adjustable parameter which will assume different values in the isotropic ( $\zeta_I$ ) and nematic ( $\zeta_N$ ) phases. This modification of the Parsons-Lee factor is the first improvement of the original theory which we propose in this work.

The final expression for the free energy  $F$  in terms of the chain length distribution  $v(l)$  is:

$$\begin{aligned} \frac{\beta F}{V} &= \sum_{l=1}^{\infty} v(l) \{ \ln[v_d v(l)] - 1 \} + \sum_{l=1}^{\infty} v(l) \sigma_o(l) \\ &+ \frac{\eta(\zeta\phi)}{2} \sum_{l=1}^{\infty} v(l) v(l') \bar{v}_{excl}(l, l') + \Delta(T) \sum_{l=1}^{\infty} (l-1) v(l) \end{aligned} \quad (12)$$

Here, we will provide an explicit expression for calculating  $\bar{v}_{excl}(l, l')$  and later on we will suggest simple analytic formulas for the isotropic and nematic phases, which are more tractable in the theoretical calculations. If we define  $\mathbf{R}_1 = \{\mathbf{r}_{1,1} \dots \mathbf{r}_{1,l}\}$ ,  $\mathbf{R}_2 = \{\mathbf{r}_{2,1} \dots \mathbf{r}_{2,l'}\}$ ,  $\mathbf{U}_1 = \{\mathbf{u}_{1,1} \dots \mathbf{u}_{1,l}\}$  and  $\mathbf{U}_2 = \{\mathbf{u}_{2,1} \dots \mathbf{u}_{2,l'}\}$ , where  $\mathbf{r}_{\gamma,i}$  and  $\mathbf{u}_{\gamma,i}$  are the position and the orientation (unit vector) of monomer  $i$  belonging to chain  $\gamma = 1, 2$ , the average excluded volume is:

$$\begin{aligned} \bar{v}_{excl}(l, l') &= -\frac{1}{V^{l+l'-1}} \int d\mathbf{R}_1 d\mathbf{R}_2 d\Omega_1 d\Omega_2 e^{ll'} \\ &(\mathbf{R}_1, \mathbf{U}_1, \mathbf{R}_2, \mathbf{U}_2) F_c(\mathbf{U}_1) F_c(\mathbf{U}_2) \end{aligned} \quad (13)$$

where  $d\mathbf{R}_\gamma = \prod_{i=1}^l d\mathbf{r}_{\gamma,i}$ ,  $d\Omega_\gamma = \prod_{i=1}^l d\omega_{\gamma,i}$  with  $d\omega_{\gamma,i}$  the infinitesimal solid angle around the orientation  $\mathbf{u}_{\gamma,i}$ ,  $e^{ll'}$  is the Mayer function [54], i.e.:

$$e^{ll'}(\mathbf{R}_1, \mathbf{U}_1, \mathbf{R}_2, \mathbf{U}_2) = \exp\{-U_h(\mathbf{R}_1, \mathbf{U}_1, \mathbf{R}_2, \mathbf{U}_2)/k_B T\} - 1, \quad (14)$$

with  $U_h(\mathbf{R}_1, \mathbf{U}_1, \mathbf{R}_2, \mathbf{U}_2)$  the hard-core pair potential:

$$U_h(\mathbf{R}_1, \mathbf{U}_1, \mathbf{R}_2, \mathbf{U}_2) = \begin{cases} \infty & \text{if } 1, 2 \text{ overlap} \\ 0 & \text{if } 1, 2 \text{ do not overlap.} \end{cases} \quad (15)$$

and  $F_c(\mathbf{U})$  is the orientational distribution function of the chain. The meaning of the prime in the integral of Equation (13) is that it has to be evaluated over all positions and orientations of monomers such that (i) within each chain only two monomers are single bonded and all the remaining monomers (if any) are double bonded<sup>1</sup> and that (ii) chains do not self-overlap. The orientational distribution function of the chain can be expressed in terms of the orientational distribution function of the monomers as follows:

$$F_c(\mathbf{U}_\alpha) = \prod_{i=1}^l f(\mathbf{u}_{\alpha,i}) \quad (16)$$

with  $\alpha = 1, 2$ .

### 3.1. Isotropic phase

In the isotropic phase the orientational distribution function of a monomer  $f(\mathbf{u})$  (where  $\mathbf{u}$  is the orientation of the monomer) in Equation (16) is uniform, i.e.:

$$f(\mathbf{u}) = \frac{1}{4\pi} \quad (17)$$

The excluded volume in Equation (13) for chains of hard cylinders can be calculated by MC integration for  $l, l' \leq 10$  and then the results can be fit to the following function:

$$v_{excl}(l, l') = 2 \left( k_I v_d \frac{l+l'}{2} + B_I X_0^2 l l' \right) \quad (18)$$

where the  $B_I$  and  $k_I$  are fitting parameters.

Under equilibrium conditions, the value of  $M$  has to minimize the free energy, i.e.

$$\frac{\partial(\beta F/V)}{\partial M} = 0 \quad (19)$$

Substituting equations (3) and (18) into (12) and calculating the sums over chain lengths, one obtains:

$$\begin{aligned} \frac{\beta F_I}{V} &= \frac{\rho}{M} \left[ \ln\left(\frac{v_d \rho}{M}\right) - 1 \right] + \rho \frac{M-1}{M} \ln(M-1) - \rho \ln M + \\ &+ \eta(\zeta_I \phi) \left[ B_I X_0^2 + \frac{v_d k_I}{M} \right] \rho^2 - \rho(\beta u_0 + \sigma_b)(1 - M^{-1}) \end{aligned} \quad (20)$$

By plugging the isotropic free energy of Equation (20) into Equation (19), one obtains the following formula:

$$M_I = \frac{1}{2} \left( 1 + \sqrt{1 + 4\phi e^{K_I \phi \eta(\phi)/v_d + \beta u_0 + \sigma_b}} \right) \quad (21)$$

which provides the isotropic average chain length  $M_I$  as a function of temperature and volume fraction.

### 3.2. Nematic phase

In the nematic phase the  $F^{or}$  contribution is different from zero and the average excluded volume takes a different form, since the orientational distribution function of monomers  $f(\mathbf{u})$  changes due to HCs alignment. The total free energy in Equation (5) is expressed as a function of the average aggregate length  $M$  and of the orientational parameter  $\alpha$ , whose equilibrium values at a given volume fraction and temperature are obtained by minimizing the free

energy. It is also assumed, as in the isotropic phase, that the chain length distribution is exponential (see Equation (3)).

For  $f(\mathbf{u})$  we adopted the form suggested many years ago by Onsager [55], i.e.:

$$f(\mathbf{u}) = f_O(\mathbf{u}) = \frac{\alpha}{4\pi \sinh \alpha} \cosh(\alpha \cos \theta) \quad (22)$$

where  $\theta$  is the angle between the monomer's symmetry axis and the nematic direction and  $\alpha$ , which controls the width of the angular distribution, is related to the nematic order parameter  $S$  as follows:

$$\begin{aligned} S &= \int_0^\pi d\theta \sin \theta \left( \frac{3}{2} \cos^2 \theta - \frac{1}{2} \right) f_O(\cos \theta) \\ &= 1 - 3 \frac{\coth \alpha}{\alpha} + \frac{3}{\alpha^2} \xrightarrow{\text{high } \alpha} 1 - \frac{3}{\alpha} \end{aligned} \quad (23)$$

As in the isotropic phase, the excluded volume in Equation (13) for chains of hard cylinders can be calculated, for different chain lengths  $l$  and value of  $\alpha$ , by MC integration of Equation (13) using the Onsager orientational distribution function  $f_O(\mathbf{u})$  (see Equation (22)) and then the results can be fit to the following function:

$$v_{\text{excl}}(l, l', \alpha) = 2 \left[ k_N(\alpha) v_d \frac{l+l'}{2} + B_N(\alpha) X_0^2 l l' \right] \quad (24)$$

where the parameters  $k_N$  and  $B_N$  are now functions of  $\alpha$ . As in Ref [34], the functional forms adopted for  $k_N(\alpha)$  and  $B_N(\alpha)$  are:

$$k_N(\alpha) = k_N^{HC}(\alpha) \quad (25)$$

$$B_N(\alpha) = \frac{\pi}{4} D^3 \left( \eta_1 + \frac{\eta_2}{\alpha^{1/2}} + \frac{\eta_3}{\alpha} \right) \quad (26)$$

where the term  $2v_d k_N^{HC}(\alpha)$  is the end-midsection contribution (i.e. the term which scales as  $l$ ) to the excluded volume of two hard cylinders which is known analytically (see Ref [36].) and  $\eta_k$  with  $k = 1, 2, 3$  are fitting parameters.

The excluded volume  $v_{\text{excl}}(l, l', \alpha)$  is calculated numerically by generating  $N_{\text{trial}}$  pairs of chains of length  $l$  (for more details see Refs [35,36]) in a box of volume  $V$ , where monomer orientations were randomly extracted from the Onsager distribution in Equation (22) for a given  $\alpha$ .

With such procedure, if  $N_{\text{overlap}}$  is the number of times that the two generated chains overlap, the excluded volume is:

$$v_{\text{excl}}(l, \alpha) = \frac{N_{\text{overlap}}}{N_{\text{trial}}} V. \quad (27)$$

The excluded volume  $v_{\text{excl}}$  is calculated for several values of  $\alpha$  ranging from 10 to 45, and  $l$  ranging from 1 to 5 and by fitting Equation (24) to these numerical estimates of  $v_{\text{excl}}$  for different  $l$  and  $\alpha$ , we determined  $\eta_i$  and thus

$B_N(\alpha)$ . In Equation (24) we implicitly assume that all aggregates, independently from their length, are nematic with the same orientational distribution function, since  $\alpha$  is independent of  $l$ . A better approach would be to introduce an  $l$ -dependent  $\alpha$ , although this way theoretical calculations would become rather demanding. A simpler strategy consists in assuming short aggregates with  $l < l_{\text{iso}}$  (in the present case  $l_{\text{iso}} = 2$ ) isotropic and all other aggregates with  $l \geq l_{\text{iso}}$  nematic with the same orientational distribution (i.e. with the same  $\alpha$ ). According to this simplifying assumption a correction term has to be calculated and added to the free energy as discussed in Ref [35].

Finally, the term  $F^{or}$  has to be evaluated. At present there is no exact analytic expression for this term, but there exist the following two analytic expressions of  $\sigma_o$  for the limiting cases of very stiff (RC) and very flexible (FC) chains [35,36,43,56, 7], i.e. when  $l \gg l_p$  (where  $l_p$  is the persistence length) and  $l \ll l_p$  respectively:

$$\begin{aligned} \sigma_o(l) &= \frac{l}{8l_p} \int \left( \frac{\partial f}{\partial \theta} \right)^2 f^{-1} d\Omega - 2 \ln \left[ \int f^{1/2} d\Omega \right] \\ &+ \ln(4\pi) \quad (l_p \ll l) \end{aligned} \quad (28)$$

$$\begin{aligned} \sigma_o(l) &= \int f \ln(4\pi f) d\Omega + \frac{l}{12l_p} \int \left( \frac{\partial f}{\partial \theta} \right)^2 f^{-1} d\Omega \\ &(l_p \gg l) \end{aligned} \quad (29)$$

By plugging into Equations (28) and (29) the exponential chain length distribution, as in Equation (3), and the Onsager orientational distribution function, and carrying out the calculations one obtains the following limiting expressions for  $\sigma_o$ :

$$\sigma_o^{RC}(l) = \log(\alpha) - 1 + \frac{\alpha - 1}{6l_p} l \quad \alpha l \ll l_p \quad (30)$$

$$\sigma_o^{FC}(l) = \log(\alpha/4) + \frac{\alpha - 1}{4l_p} l \quad \alpha l \gg l_p \quad (31)$$

As discussed in detail in Ref [35], the orientational contribution  $F^{or}$  to free energy can be expressed as the sum of contributions having the form of either one or the other of the two limiting expressions RC and FC, i.e.

$$\begin{aligned} F^{or} &= V \beta^{-1} \sum_{l=1}^{l=l_0-1} v(l) \left\{ [\log(\alpha) - 1] + \frac{\alpha - 1}{6l_p} l \right\} \\ &+ \sum_{l=l_0}^{l=\infty} v(l) \left\{ \log(\alpha/4) + \frac{\alpha - 1}{4l_p} l \right\} \end{aligned} \quad (32)$$

where the contribution of chains of length  $l < l_0$  is treated with the *RC* approximation, while the contribution of longer chains enters with the *FC* expression. The persistence length  $l_p$  for the present model have been already evaluated in Ref [34], while the details on the numerical procedure adopted for its calculation can be found in Ref [35].

In the original formulation of the theory, the parameter  $l_0$  – of the order of the persistence length  $l_p$  – was fixed and conveniently adjusted depending on the specific model used in the calculations [35,36,39]. Anyway, in Ref [41], it has been observed that, according to Ref [43,57],  $l_0$  has to be related to the deflection length  $\lambda = l_p/\alpha$ , rather than to the persistence length  $l_p$ . The rationale behind this is that bending fluctuations make linear aggregates effectively more flexible on increasing  $\alpha$ , since they are more significant if  $\alpha$  is large, i.e. if monomers are more aligned. Hence, following the same approach of Ref [41], we set  $l_0(\alpha) = \xi\lambda = \xi l_p/\alpha$ , where  $\xi$  is an adjustable parameter, which, as in Ref [41], is set equal to 0.29.

In summary, the free energy in the nematic phase can be written as follows:

$$\begin{aligned} \frac{\beta F_N}{V} = & \frac{\rho}{M} \left[ \ln\left(\frac{v_d \rho}{M}\right) - 1 \right] + \rho \frac{M-1}{M} \ln(M-1) - \rho \ln M \\ & + \eta(\zeta_N \phi) \left[ B_N X_0^2 + \frac{v_d k_N}{M} \right] \rho^2 + -\rho(\beta u_0 + \sigma_b) \left( 1 - \frac{1}{M} \right) \\ & + \sum_{l=1}^{l_0-1} v(l) \left\{ [\log(\alpha) - 1] + \frac{\alpha - 1}{6l_p} l \right\} \\ & + \sum_{l=l_0}^{\infty} v(l) \left\{ \log(\alpha/4) + \frac{\alpha - 1}{4l_p} \right\} \end{aligned} \quad (33)$$

If we assume that the orientational entropy  $\sigma_o$  can be approximated by the expression in Equation (31) valid for long chains, minimization with respect to  $M$  yields:

$$M_N = \frac{1}{2} \left( 1 + \sqrt{1 + \alpha \phi e^{K_N(\alpha) \phi \eta(\phi) / v_d + \beta u_0 + \sigma_b}} \right) \quad (34)$$

while if Equation (30) valid for short chains is assumed, one obtains:

$$M_N = \frac{1}{2} \left( 1 + \sqrt{1 + 4\alpha \phi e^{K_N(\alpha) \phi \eta(\phi) / v_d + \beta u_0 + \sigma_b - 1}} \right) \quad (35)$$

### 3.3. Phase coexistence

Coexistence lines can be calculated by imposing the conditions of equal pressure and chemical potential in the isotropic and in the nematic phase, along with the requirements that the free energy of isotropic phase in Equation (20) is minimum with respect to isotropic

average chain length  $M_I$  and that the free energy of nematic phase in Equation (33) is minimum with respect to both the nematic average chain length  $M_N$  and the parameter  $\alpha$ . These conditions translate into the following set of equations:

$$\frac{\partial F_I(\rho_I, M_I)}{\partial M_I} = 0 \quad (36)$$

$$\frac{\partial F_N(\rho_N, M_N, \alpha)}{\partial M_N} = 0 \quad (37)$$

$$\frac{\partial F_N(\rho_N, M_N, \alpha)}{\partial \alpha} = 0 \quad (38)$$

$$P_I(\rho_I, M_I) = P_N(\rho_N, M_N, \alpha) \quad (39)$$

$$\mu_I(\rho_I, M_I) = \mu_N(\rho_N, M_N, \alpha) \quad (40)$$

where  $I$  stands for isotropic and  $N$  for nematic and  $\rho_I$  and  $\rho_N$  are the number densities of the isotropic and nematic phase respectively. In the calculation of phase boundaries we had to adjust the values of  $\zeta_I$  and  $\zeta_N$  to 1.075 and 1.165 to best match theoretical predictions with numerical results. As already observed, the modified PL approach has been introduced to account for the larger effective volume occupied by each aggregate, hence it is reassuring that optimal values both for  $\zeta_I$  and  $\zeta_N$  are greater than 1.

## 4. Results and discussion

For the model discussed in Sec. 2, by using the revised theoretical approach, we calculated the phase boundaries in the  $\phi$ - $T$  plane, which are shown in Figure 2 (Th. Revised) together with the results obtained by the original version of the theory (Theory) as reported in Ref [34].

In this figure, results from MC simulations reported in Ref [34]. are also shown. Since on increasing  $T$  chains on average are shorter (as it can be evinced from Equations (21) and (34)), thus reducing the driving force for nematization, the volume fractions of both the isotropic and nematic phases at coexistence are expected to increase as shown in Figure 2. In this figure it can be seen that the revised version of theory captures much better the isotropic branch of the phase boundaries and the accuracy of the nematic branch is improved as well.

If the phase diagram in the  $\phi$ - $MX_0$  plane is considered as shown in Figure 3, similar conclusions can be drawn, even though the improvement is much less apparent.

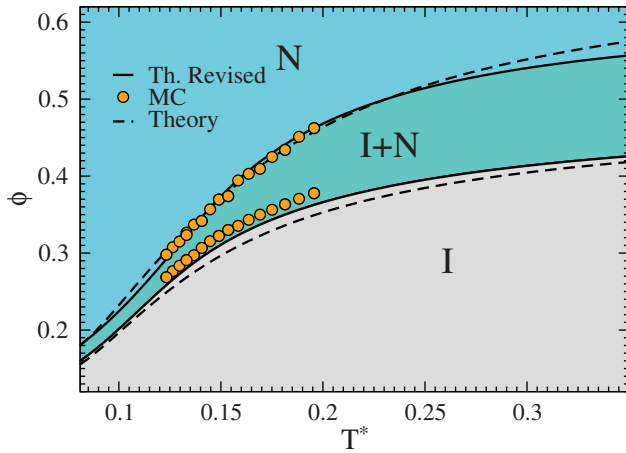


**Figure 2.** (Colour online) Isotropic-nematic phase diagram in the packing-fraction  $\phi$  vs temperature  $T^*$  plane. Circles are results from MC simulations from Ref [34]. Straight lines indicate theoretical predictions according to the present revised version of the theory. Dashed line are theoretical predictions from Ref [34], which were obtained by the original version of the theory.

The theoretical isotropic branch of the revised theory is closer to numerical results from MC simulations, although the nematic branch at higher volume fractions underestimates the numerical results to the same extent at which the original theory overestimates them.

An interesting feature of the phase diagram in the  $\phi$ - $MX_0$  plane is the reentrant (non-monotonic) behavior of the nematic branch of the phase boundaries. We note that Onsager theory predicts a monotonic behavior of both branches [34], hence this non-

monotonic behavior is a distinctive feature of self-assembly-driven nematic liquid crystals. Nevertheless, self-assembly alone is not enough to guarantee the emergence of the reentrance, since it is crucial to accurately calculate the excluded volume between polymers. Indeed, as shown in Figure 5(b) of Ref [34], the results predicted by Lu and Kindt's theory [58] and the ones from the work of Kuriabova et al. [49] do not exhibit the reentrant behavior of the phase diagram in the  $\phi - X_0M$  plane.

If one introduces the ratio  $\mathcal{R}$  between the average chain length of the nematic phase and that of the isotropic phase, i.e.

$$\mathcal{R} = M_N/M_I \quad (41)$$

this quantity at coexistence strongly depends on packing fraction through an entropic contribution related to the orientational order in the system.

At high temperatures nematization takes place at large  $\phi$  and from Equations (21) and (34) one has:

$$\mathcal{R} = \frac{M_N}{M_I} \approx \sqrt{\alpha} \quad (42)$$

According to Equation (22) the width of the orientational distribution of monomers is controlled by  $\alpha$ , hence  $\alpha$  is expected to increase dramatically at large  $\phi$ , thus making  $\mathcal{R}$  very large. At the same time, at large volume fractions  $M_I \approx 1$  [35], hence from Equation (42) it follows that  $M_N$  is also very large. Likewise, at low temperatures from Equations (21) and (34) one has that [36]:

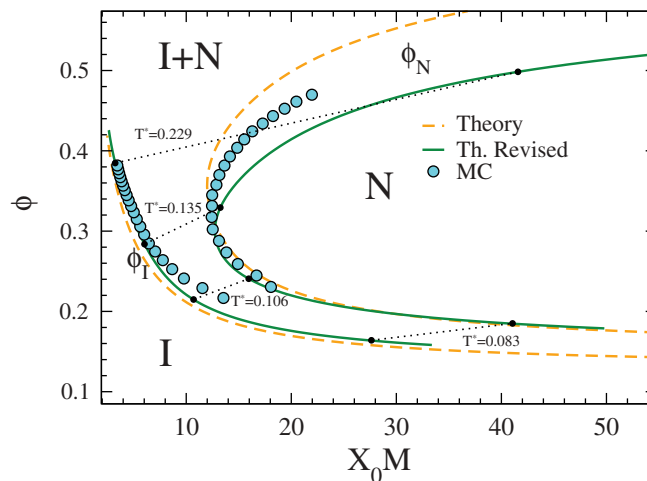


**Figure 3.** (Colour online) Isotropic-nematic coexistence lines in the average aspect ratio  $X_0M$  and volume fraction  $\phi$  plane. Symbols are numerical results from MC simulations of Ref [34]. Solid lines are theoretical predictions from the present revised version of the theory, while dashed lines are original theoretical predictions as found in Ref [34]. Full circles along the isotropic ( $\phi_I$ ) and nematic ( $\phi_N$ ) phase boundaries, which are joined by dotted lines, indicate  $\phi$  and  $M$  for isotropic and nematic phases at coexistence at the same temperature.



$$M_N \propto \sqrt{e^{\beta u_0}}, \quad (43)$$

which can increase unbounded. We deduce that  $M_N$  can reasonably exhibit a minimum as a function of  $\phi$ , i.e. a reentrant behavior as shown in Figure 2.

We note that the reentrant behavior of the nematic branch has been by now robustly confirmed by both theoretical predictions and simulations but it still awaits an experimental confirmation. The revised version of the theory of self-assembly-driven liquid crystals embodies two improvements: (i) the  $\alpha$  dependence of  $l_0$  and (ii) the use of a modified PL factors. In order to assess the relative role of these two improvements, in Figure 4 we show the phase boundaries where both improvements are used (Th. Revised) and where only the modified PL factors are used (Th. Revised PL) with  $l_0$  fixed and equal to 4 (i.e. the value used in Ref [34]). Resorting only to the modified PL factors the isotropic branch of the phase boundaries is almost unchanged while the nematic branch is clearly a bit off from MC results. If we switch to the phase diagram in the  $\phi$ - $MX_0$  plane, we have a similar situation where the nematic branch overestimates the numerical results and the isotropic branch is even closer to MC results than the full revised version of the theory. We can conclude that the modified PL factors mostly affect the isotropic branch while the nematic branch is mostly controlled by the  $\alpha$  dependence of  $l_0$ . In other words, both improvements surely matter in predicting correct results.

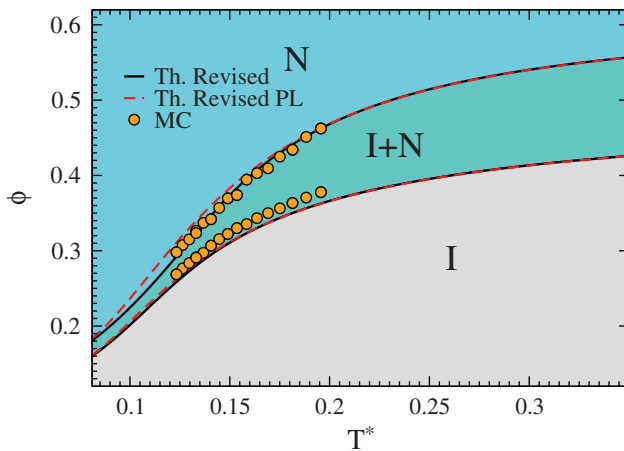


**Figure 4.** (Colour online) Isotropic-nematic phase diagram in the packing-fraction  $\phi$  vs temperature  $T^*$  plane. Symbols and lines as in Figure 2 except that dashed lines are now theoretical predictions from the revised version of the theory, where only the modified Parsons-Lee approximation is used and  $l_0 = 4$  (i.e.  $l_0$  is kept fixed and does not depend on  $\alpha$ ).

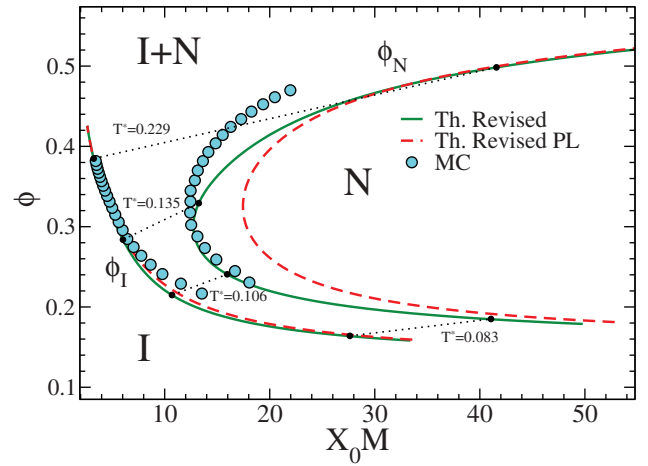


**Figure 5.** (Colour online) Isotropic-nematic coexistence lines in the average aspect ratio  $X_0M$  and volume fraction  $\phi$  plane. Symbols and lines as in Figure 3 except that the dashed lines are now theoretical predictions from the revised version of the theory where only the modified Parsons-Lee approximation is used and  $l_0 = 4$  (i.e.  $l_0$  is kept fixed and does not depend on  $\alpha$ ).

## 5. Conclusions

In this paper we proposed two possible improvements of the theory developed in Ref [35] for hard cylinder-like particles: (i) the use of a modified PL factor and (ii) the introduction of a  $\alpha$ -dependent  $l_0$  parameter. The predictions from the original theory were also compared against MC simulations of hard cylinder in Ref [34]. In this work, we compare novel predictions from the revised theory against simulations and original theoretical results, providing evidence of a significant improvement. Modeling of orientational entropy is still based on the two limiting expressions for rigid and flexible rods proposed many years ago by Khokhlov and Semenov [43,56,59], where the threshold separating the two regimes  $l_0$  is now  $\alpha$ -dependent to account for bending fluctuations [57]. A better description of the intermediate regime instead of resorting to an  $\alpha$ -dependent  $l_0$  would be advisable to have a better description of this contribution. On the other hand, a better estimate of the isotropic branch could be achieved by a better treatment of higher order terms in the virial expansion, which are at present accounted for by the PL factor. In the present version of the theory two adjustable parameters are introduced in the modified PL factors of the isotropic and nematic phases and they have been adjusted to maximize the agreement between theory and simulations. A future goal would be to avoid the use of adjustable parameters by a suitable microscopic treatment of the higher order contributions to the virial expansion. Despite the limitations of the present approach, where these two

parameters have to be adjusted ad-hoc for a given model, the importance of the present findings relies on the fact that they clearly point towards the need of going beyond the PL decoupling approximation.

A further improvement of the theory would be to employ a joint orientation and chain length distribution, as suggested first for non self-assembling systems by van der Schoot and Cates [6,46]. A first attempt in this direction has been done in Ref [49] and the present approach can be modified accordingly. A possible simpler strategy would be to introduce an  $l$ -dependent  $\alpha$ . In Ref [38], where bifunctional hard spheres are studied, it has been observed that if the theory accounts for the  $l$ -dependence of  $\alpha$ , the nematic phase is expected to be favored against the isotropic phase, thus resulting in a wider coexistence region, i.e. an isotropic branch closer to numerical results. Although theoretical calculations become rather demanding and cumbersome by introducing an  $l$ -dependent  $\alpha$ , the residual gap found between theoretical predictions and numerical results, as shown in Figure 1, could possibly be filled this way.

## Note

1. The only exception is when we have two chains, each constituted of two monomers.

## Disclosure statement

No potential conflict of interest was reported by the author.

## References

- [1] Glotzer SC. Some assembly required. *Science*. 2004;306:419–420.
- [2] Hamley IW. Introduction to soft matter. West Sussex, England: Wiley & Sons; 2007.
- [3] Whitesides GM, Boncheva M. Beyond molecules: self-assembly of mesoscopic and macroscopic components. *Proc Natl Acad Sci USA*. 2002;99(8):4769–4774.
- [4] Khan A. Phase science of surfactants. *Curr Opin Colloid Interface Sci*. 1996;1:614.
- [5] Kuntz DM, Walker LM. Nematic phases observed in amphiphilic polyelectrolyte-surfactant aggregate solutions. *Soft Matter*. 2008;4:286–293.
- [6] van der Schoot P, Cates ME. Growth, static light scattering, and spontaneous ordering of rodlike micelles. *Langmuir*. 1994;10:670–679.
- [7] Aggeli A, Bell M, Carrick LM, et al.  $\beta$  as a trigger of peptide  $\beta$ -sheet self-assembly and reversible switching between nematic and isotropic phases. *J Am Chem Soc*. 2003;125(32):9619–9628.
- [8] Ciferri A. On collagen ii fibrillogenesis. *Liq Cryst*. 2007;34(6):693–696.
- [9] Lee CF. Isotropic-nematic phase transition in amyloid fibrilization. *Phys Rev E*. 2009;80(3):031902.
- [10] Mezzenga R, Jung J-M, Adamcik J. Effects of charge double layer and colloidal aggregation on the isotropic-nematic transition of protein fibers in water. *Langmuir*. 2010;26(13):10401–10405.
- [11] Cortini R, Cheng X, Smith JC. The tilt-dependent potential of mean force of a pair of DNA oligomers from all-atom molecular dynamics simulations. *J Phys Condens Matter*. 2017 jan;29(8):084002.
- [12] Fraccia TP, Smith GP, Clark NA, et al. Liquid crystal ordering of four-base-long DNA oligomers with both G–C and A–T pairing. *Crystals*. 2017;8(1):5.
- [13] Di Leo S, Todisco M, Bellini T, et al. Phase separations, liquid crystal ordering and molecular partitioning in mixtures of PEG and DNA oligomers. *Liq Cryst*. 2018;45(13–15):2306–2318.
- [14] Maffeo C, Luan B, Aksimentiev A. End-to-end attraction of duplex DNA. *Nucl Acids Res*. 2012;40(9):3812–3821.
- [15] Nakata M, Zanchetta G, Chapman BD, et al. End-to-end stacking and liquid crystal condensation of 6 to 20 base pair DNA duplexes. *Science*. 2007;318:1276.
- [16] Salamonczyk M, Zhang J, Portale G, et al. Smectic phase in suspensions of gapped DNA duplexes. *Nat Commun*. 2016;7(11):13358.
- [17] Saurabh S, Lansac Y, Jang YH, et al. Understanding the origin of liquid crystal ordering of ultrashort double-stranded DNA. *Phys Rev E*. 2017 Mar;95:032702.
- [18] Smith GP, Fraccia TP, Todisco M, et al. Backbone-free duplex-stacked monomer nucleic acids exhibiting Watson–Crick selectivity. *Proc Natl Acad Sci*. 2018;115(33):E7658–E7664.
- [19] Livolant F, Levelut AM, Doucet J, et al. The highly concentrated liquid-crystalline phase of DNA is columnar hexagonal. *Nature*. 1989;339(6227):724–726.
- [20] Merchant K, Rill RL. DNA length and concentration dependencies of anisotropic phase transitions of dna solutions. *Biophys J*. 1997;73(6):3154–3163.
- [21] Robinson C. Liquid-crystalline structures in polypeptide solutions. *Tetrahedron*. 1961;13(1–3):219–234.
- [22] Tombolato F, Ferrarini A. From the double-stranded helix to the chiral nematic phase of B-DNA: A molecular model. *J Chem Phys*. 2005;122(5):054908.
- [23] Chami F, Wilson MR. Molecular order in a chromonic liquid crystal: A molecular simulation study of the anionic azo dye sunset yellow. *J Am Chem Soc*. 2010;132:7794–7802.
- [24] Edwards RG, Henderson JR, Pinning RL. Simulation of self-assembly and lyotropic liquid crystal phases in model discotic solutions. *Mol Phys*. 1995;86(4):567–598.
- [25] Henderson JR. Discotic amphiphiles. *J Chem Phys*. 2000;113(14):5965–5970.
- [26] Lydon J. Chromonic liquid crystalline phases. *Liq Cryst*. 2011;38(11–12):1663–1681.
- [27] Maiti PK, Lansac Y, Glaser MA, et al. Isodesmic self-assembly in lyotropic chromonic systems. *Liq Cryst*. 2002;29(5):619–626.
- [28] Park H-S, Kang L, Tortora S-W, et al. Self-assembly of lyotropic chromonic liquid crystal sunset yellow and

- effects of ionic additives. *J Phys Chem B*. 2008;112(51):16307–16319.
- [29] Zhou S, Nastishin YA, Omelchenko MM, et al. Elasticity of lyotropic chromonic liquid crystals probed by director reorientation in a magnetic field. *Phys Rev Lett*. 2012;109:037801.
- [30] Horsch MA, Zhang Z, Glotzer SC. Self-assembly of polymer-tethered nanorods. *Phys Rev Lett*. 2005 Jul;95:056105.
- [31] Horsch MA, Zhang Z, Glotzer SC. Self-assembly of laterally-tethered nanorods. *Nano Lett*. 2006;6(11):2406–2413.
- [32] Liu K, Nie Z, Zhao N, et al. Step-growth polymerization of inorganic nanoparticles. *Science*. 2010;329(5988):197–200.
- [33] Liu K, Zhao N, Kumacheva E. Self-assembly of inorganic nanorods. *Chem Soc Rev*. 2011;40:656–671.
- [34] Nguyen KT, Sciortino F, De Michele C. Self-assembly-driven nematization. *Langmuir*. 2014;30:4814–4819.
- [35] De Michele C, Bellini T, Sciortino F. Self-assembly of bifunctional patchy particles with anisotropic shape into polymers chains: theory, simulations, and experiments. *Macromolecules*. 2012;45(2):1090–1106.
- [36] De Michele C, Rovigatti L, Bellini T, et al. Self-assembly of short DNA duplexes: from a coarse-grained model to experiments through a theoretical link. *Soft Matter*. 2012;8:8388–8398.
- [37] Nguyen KT, Battisti A, Ancora D, et al. Self-assembly of mesogenic bent-core DNA nanoduplexes. *Soft Matter*. 2015;11:2934–2944.
- [38] Nguyen KT, De Michele C. Nematic liquid crystals of bifunctional patchy spheres. *Eur Phys J E*. 2018;41(12):141.
- [39] Romani E, Ferrarini A, De Michele C. Elastic constant of chromonic liquid crystals. *Macromolecules*. 2018;51:5409–5419.
- [40] De Michele C, Zanchetta G, Bellini T, et al. Hierarchical propagation of chirality through reversible polymerization: the cholesteric phase of DNA oligomers. *ACS Macro Lett*. 5:208–212, 2016.
- [41] Bagnani M, Nyström G, De Michele C, et al. Amyloid fibrils length controls shape and structure of nematic and cholesteric tactoids. *ACS Nano*. 2019;13(1):591–600.
- [42] Milchev A, Egorov SA, Binder K, et al. Nematic order in solutions of semiflexible polymers: hairpins, elastic constants, and the nematic-smectic transition. *J Chem Phys*. 2018;149(17):174909.
- [43] Odijk T. Theory of lyotropic polymer liquid crystals. *Macromolecules*. 1986;19:2313–2329.
- [44] Henderson JR. Concentration dependence of linear self-assembly and exactly solvable models concentration dependence of linear self-assembly and exactly solvable models. *Phys Rev Lett*. 1996;77(11):2316–2319.
- [45] Henderson JR. Physics of isodesmic chemical equilibria in solution. *Phys Rev E*. 1997;55(5):5731–5742.
- [46] van der Schoot P, Cates ME. The isotropic-to-nematic transition in semi-flexible micellar solutions. *Europhys Lett*. 1994;25:515–520.
- [47] Lee SD. A numerical investigation of nematic ordering based on a simple hard-rod model. *J Chem Phys*. 1987;87:4972–4974.
- [48] Parsons JD. Nematic ordering in a system of rods. *Phys Rev A*. 1979;19:1225–1230.
- [49] Kuriabova T, Betterton MD, Glaser MA. Linear aggregation and liquid-crystalline order: comparison of monte carlo simulation and analytic theory. *J Mater Chem*. 2010;20:10366–10383.
- [50] Sciortino F, Bianchi E, Douglas JF, et al. Self-assembly of patchy particles into polymer chains: A parameter-free comparison between wertheim theory and monte carlo simulation. *J Chem Phys*. 2007;126:194903.
- [51] Tortora MMC, Doye JPK. Perturbative density functional methods for cholesteric liquid crystals. *J Chem Phys*. 2017;146(18):184504.
- [52] Tortora MMC, Doye JPK. Incorporating particle flexibility in a density functional description of nematics and cholesterics. *Mol Phys*. 2018;116(21–22):2773–2791.
- [53] Varga S, Szalai I. Modified parsons-lee theory for fluids of linear fused hard sphere chains. *Molec. Phys.*, 98:693–698, 2000.
- [54] McQuarrie DA. *Statistical mechanics*. Sausalito, CA: University Science Books; 2000.
- [55] Onsager L. The effects of shape on the interaction of colloidal particles. *Ann N Y Acad Sci*. 1949;51:627–659.
- [56] Khokhlov AR, Semenov AN. Liquid-crystalline ordering in the solution of partially flexible macromolecules. *Physica*. 1982;112A:605–614.
- [57] Odijk T. Pitch of a polymer cholesteric. *J Phys Chem*. 1987;91:6060–6062.
- [58] Lü X, Kindt JT. Monte carlo simulation of the self-assembly and phase behavior of semiflexible equilibrium polymers. *J Chem Phys*. 2004;120:10328–10338.
- [59] Vroege GJ, Lekkerkerker HNW. Phase transitions in lyotropic colloidal and polymer liquid crystals. *Rep Prog Phys*. 1992;55:1241–1309.